Entanglement Dynamics in the Jaynes-Cummings Model

Author: Nicolás Landa Baila, nlandaba40@alumnes.ub.edu
Facultat de Física, Universitat de Barcelona, Diagonal 645, 08028 Barcelona, Spain.

Advisor: Maria Moreno Cardoner, maria.moreno@fqa.ub.edu

Abstract: Entanglement lies at the heart of quantum technologies, enabling quantum computation, secure communication, and ultra-precise sensing, and it arises naturally in systems of atoms interacting with light. In this work, we analyze the entanglement dynamics resulting from the interaction between a two-level atom and a single quantized mode of the electromagnetic field, described by the paradigmatic Jaynes–Cummings Hamiltonian. By preparing the system initially in different field states, including Fock, coherent, and squeezed vacuum states, we compute the corresponding time evolution and quantify the entanglement generated between atom and light using the concept of bipartite entanglement entropy. Our results show how photon statistics influence both the generation and the stability of entanglement.
Keywords: Quantum many-body physics, Electromagnetic field, Hilbert space, Superposition principle, Hamiltonian, Entropy.
SDGs: (4) Quality Education, (9) Industry, Innovation and Infrastructure, (13) Climate action.

I. INTRODUCTION

Understanding how atoms and light interact at the quantum level is crucial for many current quantum technologies where atoms are used for storing and processing information while photons are ideal carriers for transmitting it. One of the simplest and most representative models describing such interactions is the Jaynes-Cummings Hamiltonian [1], describing a simple quantum emitter interacting with a single quantized electromagnetic mode, allowing the observation of purely quantum phenomena such as coherent excitation exchange and the generation of entanglement between light and matter.

This model has been experimentally realized in multiple platforms, including Rydberg atoms in microwave [2, 4] and optical [5] cavities, trapped ions [3], and more recently, superconducting qubits [6], and quantum dots [7]. These investigations were recognized with the Nobel Prize in Physics in 2012, awarded to Haroche and Wineland for their pioneering work in manipulating individual quantum systems.

The entanglement generated in these systems is not only a clear manifestation of the quantum nature of light–matter interactions, but also an essential resource for quantum information tasks such as computation, communication, and sensing. In the Jaynes–Cummings model, the entanglement between atom and light can be quantified using the von Neumann entropy of the atomic reduced density matrix [8]. While the global atom-field system evolves unitarily and remains pure, the atomic subsystem typically becomes mixed, signaling the emergence of correlations and entanglement with the field.

In this work, we analyze the time evolution of entanglement between a single two-level atom and a single quantized mode of the electromagnetic field, initially uncorrelated. We study how the choice of the initial state of the field -whether a Fock, coherent, or squeezed vacuum state- influences the dynamics of entanglement.

II. THEORETICAL FRAMEWORK

Let us consider a two-level quantum emitter (qubit), with energy levels $|g\rangle$ and $|e\rangle$, which is coupled to a single quantized electromagnetic mode, such as the optical mode of a high-finesse cavity (see Fig. 1). This can be described by the Jaynes-Cummings Hamiltonian [1], which in the rotating-wave approximation that neglects energy non-conserving terms, takes its simplest form (from now on $\hbar = 1$):

$$H = \omega_0 \sigma^\dagger \sigma + \omega a^\dagger a + g(\sigma a^\dagger + \sigma^\dagger a). \tag{1}$$

Here, $\sigma = |g\rangle\langle e|$ and $\sigma^\dagger = |e\rangle\langle g|$ are, respectively, the annihilation and creation operators of an atomic excitation, while a and $a^\dagger$ are the annihilation and creation operators associated with the field. They act on a n-photon state according to $a|n\rangle = \sqrt{n}|n-1\rangle$ and $a^\dagger|n\rangle = \sqrt{n+1}|n+1\rangle$. We denote by ω and ω_0 the field and atomic transition frequencies, and g the atom-photon coupling strength.

We will work in the Fock basis of the composite system, where each basis state is of the form $|\eta, n\rangle$, with $\eta \in \{g, e\}$ denoting the atomic state, and $n \in \mathbb{N}_0$ the number of photons. In numerical implementations we will truncate the basis to a sufficiently large N to ensure all relevant contributions are accounted for.

The conservation of the total number of excitations allows the Hilbert space to be decomposed into finite-dimensional subspaces (blocks), simplifying the analysis of the system dynamics. In particular, the Hamiltonian Eq. (1) only couples states of the form $|g, n\rangle \leftrightarrow |e, n-1\rangle$ and thus decomposes into independent 2×2 blocks acting on these two-dimensional subspaces. Each block has the form:

$$H_n = \begin{pmatrix} n\omega & g\sqrt{n} \\ g\sqrt{n} & n\omega - \Delta \end{pmatrix}, \tag{2}$$

where $\Delta = \omega - \omega_0$ is the detuning between the field and

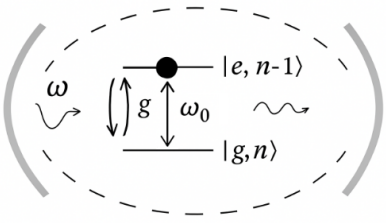

FIG. 1: Schematics of the system. A single two-level quantum emitter (with levels $|g\rangle$ and $|e\rangle$) couples with strength g to a single light mode (such as a cavity mode). The atomic and light frequencies are denoted by ω_0 and ω, respectively.

the atomic frequency. This reduces the full dynamics to a sequence of simple two-level systems.

Bipartite Entanglement.— One of the main goals of this work is to quantify the entanglement generated between atoms and photons. Entanglement is a property of a composite system in which the quantum state of the whole system cannot be written as a product of the states of its parts. More precisely, let us consider a bipartite system with subsystems A and B, whose Hilbert space can be written as $\mathcal{H}_A \otimes \mathcal{H}_B$. A pure state $|\Psi\rangle$ is entangled when it cannot be written in the form $|\Psi\rangle = |\Phi\rangle_A|\xi\rangle_B$, where $|\Phi\rangle_A$ and $|\xi\rangle_B$ are states of the corresponding Hilbert spaces $\mathcal{H}_A$ and $\mathcal{H}_B$.

Given this partition, we can construct the reduced density matrix of subsystem A as $\rho_A = \mathrm{Tr}_B(\rho)$, where ρ is the density matrix of the total system and the trace is performed over the degrees of freedom of subsystem B. Equivalently, the reduced density matrix of subsystem B is $\rho_B = \mathrm{Tr}_A(\rho)$. For a pure state, the bipartite entanglement between A and B can be quantified using the entanglement entropy, which is defined as the von Neumann entropy of any of the two reduced density matrices:

$$S(\rho_A) = -\mathrm{Tr}(\rho_A \log \rho_A) = -\mathrm{Tr}(\rho_B \log \rho_B) = S(\rho_B). \tag{3}$$

This quantity vanishes for a state with no entanglement. Indeed, in this case, the reduced density matrix in the basis in which the state is a product state is diagonal with only a single non-zero eigenvalue equal to one.

In this work, we choose A to be a single qubit and B the light field. Thus, S quantifies the amount of entanglement between atom and light.

III. RESULTS: FOCK STATE INITIALIZATION

We start with the simplest case of an initial state being a Fock state. We choose that the atom is initially in the excited state, while the cavity contains no photons. This corresponds to a product state of the composite system $|\psi(t=0)\rangle = |e,0\rangle$ with no entanglement and a total excitation number equal to one. The dynamics are thus restricted to the subspace generated by the two states $|e,0\rangle$ and $|g,1\rangle$, and therefore entirely contained within the H_1 block introduced in Eq. (2).

The diagonalization of H_1 yields the eigenvalues:

$$E_\pm = -\frac{\Delta}{2} \pm \frac{\Omega}{2}, \quad \Omega = \sqrt{4g^2 + \Delta^2}. \tag{4}$$

Since H is time-independent, the time evolution of the state is given by $|\Psi(t)\rangle = e^{-iH_1 t}|\Psi(t=0)\rangle$. By expressing the state in the Fock basis $|\psi(t)\rangle = c_{g,1}(t)|g,1\rangle + c_{e,0}(t)|e,0\rangle$, we find for the coefficients:

$$\begin{aligned} c_{g,1}(t) &= -i \exp\left(-i\frac{\Delta}{2}t\right) \frac{2g}{\Omega} \sin(\Omega t/2) \\ c_{e,0}(t) &= \exp\left(-i\frac{\Delta}{2}t\right) \left[\cos(\Omega t/2) - i\frac{\Delta}{\Omega}\sin(\Omega t/2)\right]. \end{aligned} \tag{5}$$

The ground and excited state populations are then given by $P_g(t) = |c_{g,1}(t)|^2$ and $P_e(t) = |c_{e,0}(t)|^2$, respectively.

Since the state $|\Psi(t)\rangle$ is always pure (it evolves unitarily), the total density matrix is directly $\rho(t) = |\psi(t)\rangle\langle\psi(t)|$. Performing the trace over the photonic degree of freedom, we obtain the atomic reduced density matrix, where only the diagonal terms survive:

$$\rho_{\mathrm{at}}(t) = \begin{pmatrix} 1 - P_e(t) & 0 \\ 0 & P_e(t) \end{pmatrix}. \tag{6}$$

Finally, the von Neumann entropy becomes:

$$S(t) = -P_e(t)\log P_e(t) - (1 - P_e(t))\log(1 - P_e(t)). \tag{7}$$

Although the expression diverges formally at $P_e = 0$ and $P_e = 1$, the entropy approaches zero in both limits. At these points the atomic state is unentangled, and we will take $S = 0$.

According to Eqs. (5), the atomic level populations exhibit oscillations known as Rabi oscillations, with a frequency and amplitude that depend on Δ and g. In the resonant case ($\Delta = 0$), where the light frequency exactly matches the atomic transition frequency, the atomic state populations oscillate with frequency $\Omega_r = 2g$ and maximal amplitude equal to 1, leading to full excitation transfer between atomic and photonic modes. Instead, the presence of detuning ($\Delta \neq 0$) reduces the oscillation amplitude by a factor Δ^2/Ω^2, while the frequency increases and is equal to $\Omega_{nr} = \sqrt{4g^2 + \Delta^2}$. These results are shown in Fig. (2).

In the same figure, we also plot the entanglement entropy evaluated from Eq. (7). This attains a global maximum at $P_e = 1/2$, with $S_{\max} = \log 2$, and vanishes for $P_e = 0$ and $P_e = 1$. Consequently, in the resonant case, the entanglement reaches its maximum when $t = (2n+1)\pi/2\Omega_r$, and vanishes at $t = n\pi/\Omega_r$ (with n being an integer), corresponding to the revival of the initial state or complete population inversion. In the off-resonant case, full population inversion does not occur, and the entanglement vanishes only at $t = 2n\pi/\Omega_{nr}$, while exhibiting local minima at $t = (2n+1)\pi/\Omega_{nr}$.

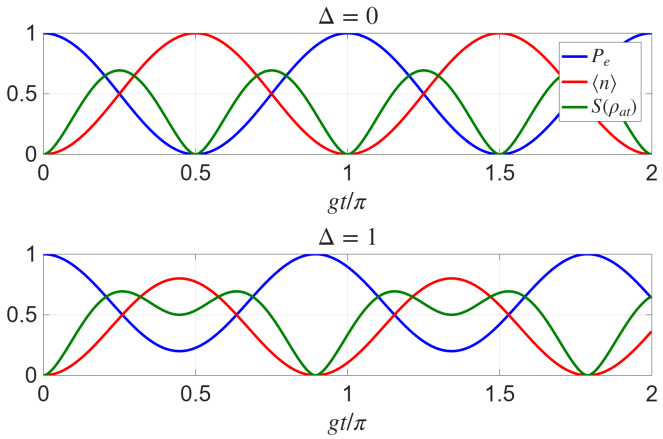

FIG. 2: Population of the $|e\rangle$ state (blue), the average number of photons (red) and the entanglement entropy S (green), for the resonant ($\Delta = 0$, top) and non-resonant ($\Delta/g = 1$, bottom) cases, plotted as a function of the dimensionless parameter gt/π. The initial state is $|e, 0\rangle$.

IV. RESULTS: COHERENT AND SQUEEZED VACUUM STATE INITIALIZATION

Having understood the dynamics restricted within one of the Hamiltonian blocks Eq. (2), we will now consider initially a more general product state $|\Psi(t=0)\rangle = |e\rangle \otimes |\Phi\rangle$, where the field state is of the general form:

$$|\Phi\rangle = \sum_{n=0}^{\infty} c_n |n\rangle. \tag{8}$$

Here, the c_n coefficients determine the probability $|c_n|^2$ to find the system with exactly n photons.

From now on, and for simplicity, we will restrict ourselves to the resonant case, and set $\Delta = 0$ in the Hamiltonian Eq. (2). We can now make a similar development to the previous section for each of the blocks, arriving at the following time evolution expression:

$$|\psi(t)\rangle = \sum_n c_n \left[-i \sin(\sqrt{n} g t)\, |g, n\rangle + \cos(\sqrt{n} g t)\, |e, n-1\rangle\right] \tag{9}$$

Performing the partial trace over the photon degree of freedom, we obtain for the reduced atomic density matrix components:

$$\rho_{\text{at}}^{ee} = \sum_{n=1}^{\infty} |c_n|^2 \cos^2(\sqrt{n} g t) \tag{10}$$

$$\rho_{\text{at}}^{ge} = \sum_{n=1}^{\infty} i c_n c_{n+1}^* e^{i\omega t} \cos(\sqrt{n+1} g t) \sin(\sqrt{n} g t), \tag{11}$$

with $\rho_{\text{at}}^{gg} = 1 - \rho_{\text{at}}^{ee}$ and $\rho_{\text{at}}^{eg} = (\rho_{\text{at}}^{ge})^*$.

Note that, in general, the atomic coherences ρ_{at}^{ge} do not vanish. This is opposite to the case of having an initial photonic Fock state. Eq. (6) is not valid here, and $S(\rho_{\text{at}})$ needs to be evaluated from Eq. (3).

A. Coherent States

We will first consider that the photonic field $|\Phi\rangle$ corresponds to a coherent state $|\alpha\rangle$. Coherent states of the electromagnetic field are fundamental in quantum optics as they are quantum states that best approximate the classical behavior of a mode of the electromagnetic field, with minimum uncertainty in any direction in phase space [9]. They are defined as eigenstates of the annihilation operator of a photon a: $a|\alpha\rangle = \alpha|\alpha\rangle$. The coefficients in the Fock basis are given by:

$$c_n = e^{-|\alpha|^2/2} \frac{\alpha^n}{\sqrt{n!}}. \tag{12}$$

The probability $p_n = |c_n|^2$ to find the system with exactly n photons follows a Poissonian distribution with average photon number $\langle n\rangle = |\alpha|^2$ and variance $\text{Var}(n) = |\alpha|^2$. For small values of $|\alpha|$, the distribution is narrow and highly non-Gaussian. However, as $|\alpha|$ increases, it tends to a Gaussian profile centered at the mean value $\langle n\rangle = |\alpha|^2$. Figure 3 (a) shows the photon number distribution for coherent states with different values of α.

Having defined the coefficients c_n, we now compute the atomic reduced density matrix and evaluate the entanglement entropy $S(\rho_{\text{at}})$ as given in Eq. (3). The result for ρ_{at}^{ee} and $|\rho_{\text{at}}^{ge}|$, together with $S(\rho_{\text{at}})$, as a function of time t and for a particular value of $\alpha = 3$ is shown in Fig. 3 (b). We also perform a sweep over a range of values of the α parameter, and compute the entanglement entropy and plot it versus α and time t in Fig. 3 (c).

These results show a more complex dynamics compared to the case of an initial photonic state with a single Fock component. They involve a superposition of harmonic functions of different frequencies $\Omega_n = \sqrt{n}\Omega$, weighted by the corresponding coefficients c_n.

The dynamics of the reduced density matrix components, as depicted in Fig. 3 (b), exhibit distinct behaviors depending on the magnitude of $|\alpha|$. In the limit $|\alpha| \ll 1$ corresponding to a mean photon number close to zero, the evolution resembles the regime analyzed in Sec. III. In this case, both, population and entanglement, display regular oscillations at frequency $\Omega_r = 2g$.

As the value of α increases, the system transitions to a qualitatively different dynamical regime characterized by the appearance of collapse and revival structure in the atomic populations. Superposed on these dynamics are fast oscillations occurring at a frequency determined by the dominant photon number component $\Omega_{\bar{n}} = 2g\sqrt{\bar{n}} = 2g\alpha$ (that is, the frequency for which the distribution is maximum). We note that for a classical field of intensity $\propto \bar{n}$, populations will perform regular oscillations at the same frequency $\Omega_{\bar{n}}$, but we will not observe collapse phenomena or entanglement generation.

Instead, for the coherent state (that is still quantum), these rapid oscillations are modulated by a slower envelope arising from differences between Rabi frequencies corresponding to adjacent photon numbers. A Taylor expansion around the dominant frequency $\Omega_{\bar{n}}$ leads to

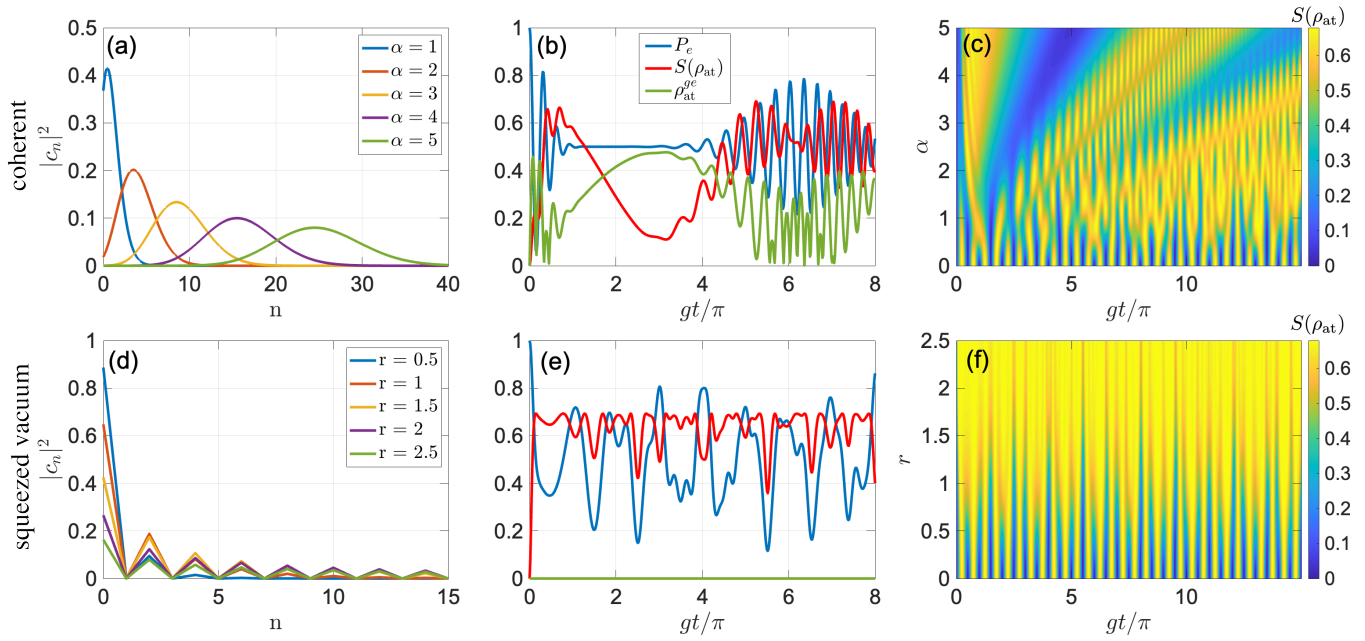

FIG. 3: Atom-field dynamics under the Jaynes-Cummings model for different initial field states: coherent (top panels) and squeezed vacuum states (bottom panels). (a) and (d) Photon number distribution $|c_n|^2$ for different values of α and r, respectively. (b) and (e) Time evolution of the excited state population $P_e = \rho^{ee}_{\rm at}$ (blue), absolute value of coherence $|\rho^{eg}_{\rm at}|$ (green) and entanglement entropy $S(\rho_{\rm at})$ (red), as a function of the dimensionless parameter gt/π. (c) and (f) Color map of $S(\rho_{\rm at})$ as a function of gt/π and α or r, respectively.

$\Omega_{\bar{n}+\delta n} \approx \Omega_{\bar{n}} + \delta n \cdot \partial\Omega_n/\partial n|_{\bar{n}} = 2\sqrt{\bar{n}}g + \delta n \cdot g/\sqrt{\bar{n}}$, where δn represents small deviations in photon number from the dominant component. Thus, we find that the dominating difference in frequency (setting in the previous expression $\delta n = 1$) is $\Delta\Omega = \Omega_{\bar{n}+\delta n} - \Omega_{\bar{n}} \approx g/\sqrt{\bar{n}} = g/\alpha$.

The interference among the different Fock components induced by these frequency differences results in a gradual suppression of the coherent oscillations, leading to the collapse phenomenon. The associated collapse time scale can be estimated as $T^{\rm col} \propto 1/\Delta\Omega = \alpha/g$. During this stage, destructive interference among the various Rabi frequencies induces a substantial increase in atom-field entanglement as reflected in the behavior of Fig. 3.

At longer times, partial revivals emerge as the dominant Fock components approximately re-phase. We expect this to occur for a time $T^{\rm rev}$ such that for the most relevant frequency components Ω_n it is fulfilled that $(\Omega_n - \Omega_{\bar{n}}) \cdot T^{\rm rev} \approx 2\pi m$ (for some m integer value). Again, if we focus on the dominating components such that $\Omega_n - \Omega_{\bar{n}} \approx \delta n \cdot g/\alpha$, we find a revival time $T^{\rm rev} = 2\pi\alpha/g$. This estimation remains only valid for the most populated states of photons, and therefore full revivals are not generally observed. Nevertheless, a decrease in the entanglement entropy $S(\rho_{at})$ is observed at these times indicating an evolution towards a state more separable.

Additionally, at times around $T^{\rm rev}/2$, a strong reduction in the entropy $S(\rho_{at})$ is observed with an increase in atomic coherence between the ground and excited states. In this regime, the atomic state closely approximates to $|\Psi\rangle \approx (|g\rangle - i|e\rangle)/\sqrt{2}$, corresponding to a nearly pure state with minimal entanglement with the field.

B. Squeezed Vacuum States

Squeezed vacuum states are a class of non-classical states of light that exhibit reduced quantum uncertainty in one field quadrature at the expense of increased uncertainty in the conjugate quadrature [10]. These states are generated by applying a squeezing operator to the vacuum and are characterized by a nontrivial photon number distribution that contains only even photon numbers and exhibits super-Poissonian statistics, that is, the variance on the photon number is larger than its mean value.

More precisely, for a single optical mode (described by a and $a^\dagger$ operators) the squeezing operator can be written as $S(\xi) = \exp(\xi^* a^2 - \xi a^{\dagger 2})$, where $\xi = re^{i\theta}$ is the squeezing parameter. Here the r parameter sets the strength of the squeezing, while the θ angle determines its direction. When applied to the electromagnetic vacuum, it leads to the squeezed vacuum state $S(\xi)|0\rangle$, creating pairs of photons with correlated phase and amplitude.

In this work we will choose $\theta = 0$, corresponding to squeezing in the position-like quadrature, defined as $\hat{X} = (a + a^\dagger)/\sqrt{2}$. This leads to a reduced variance in this operator, compared to the variance of the vacuum state or a coherent state. Since the uncertainty principle needs to be fulfilled, this also means that the variance in the conjugate quadrature (in this case the momentum-

like quadrature $\hat{P} = i(a - a^\dagger)\sqrt{2})$ will be increased (anti-squeezing). A different value of θ rotates the squeezing axis in phase space, determining which quadrature is squeezed and which is anti-squeezed.

For the $\theta = 0$ case, the coefficients c_n in the Fock decomposition take the values:

$$c_n = \begin{cases} \dfrac{1}{\sqrt{\cosh r}} \cdot \dfrac{\sqrt{n!}}{(n/2)!} \left(-\dfrac{1}{2}\tanh r\right)^{n/2}, & \text{if } n = 2k \\ 0, & \text{if } n = 2k+1, \end{cases} \tag{13}$$

where $k \in \mathbb{N}_0$.

Therefore, only even photon number components are present in this state. The mean value of photons is given by $\bar{n} = \sinh^2(r)$, while the variance $\mathrm{Var}(n) = \bar{n}(\bar{n}+1) > \bar{n}$, indicating that the distribution is broader compared to the coherent state case (now it is super-Poissionian). The corresponding probability distribution is depicted in Fig. 3 (d) as a function of photon number n for different values of the squeezing parameter r.

In this case, and from Eqs. (11) we can see that the atomic density matrix remains diagonal during the full time evolution, with coherences between the ground and the excited state identically equal to zero. Nevertheless, the atom becomes entangled with the field very quickly, reflecting the spreading of excitation amplitudes across multiple photon number components. This is shown in Fig. 3 (e) and (f).

In comparison to the coherent light field case, we do not observe in this case a collapse where the population oscillations are completely suppressed. In the case of squeezed vacuumm, dephasing is reduced, due to the peaked distribution at $n = 0$ component and a more spaced photon number components. This leads to more regular oscillations in the observables, with frequency close to the vacuum Rabi frequency $\Omega_r = 2g$.

V. CONCLUSIONS

In this work, we have studied the dynamics of the atomic state populations and the atom–photon entanglement in the Jaynes–Cummings model for three different initial field states, and have shown how they are governed by the photon-number statistics.

When the field is prepared in a single Fock state, where the photon number is sharply defined, the system exhibits perfectly periodic Rabi oscillations. In this regime, entanglement undergoes regular oscillations, reaching maximal values when the excitation is equally shared between the atom and the field, and returning to zero when the system temporarily factorizes. Since there is no uncertainty in the photon number, no coherences are present.

In contrast, for initial coherent light states, the superposition of multiple photon-number components gives rise to the canonical collapse and revival phenomenon. The initial Rabi oscillations rapidly dephase due to the spread of photon number dependent frequencies, leading to a temporary collapse of both the atomic population and the entanglement. However, constructive rephasing occurs after a characteristic revival time, and both the atomic population and entanglement are restored.

Finally, the squeezed vacuum state offers another distinct possible regime. Its even photon number distribution and super-Poissonian statistics reduce the spread of Rabi frequencies leading to more regular oscillations and prolonged entanglement.

Altogether, our results illustrate the crucial role that photon-number statistics play in determining both the population dynamics and the entanglement properties of atom–field systems. The tools developed in this work not only reproduce the well-known features of the Jaynes–Cummings model but also provide quantitative criteria for tuning and optimizing entanglement generation.

Acknowledgments

I am sincerely grateful to my advisor, Dra. Maria Moreno, whose guidance and commitment were fundamental in the development of this work, and deeply thankful to my parents for their wholehearted support.

[1] E. T. Jaynes and F. W. Cummings, Proceedings of the IEEE, **51**, 89-109 (1963).
[2] M. Brune, J. M. Raimond, P. Goy, L. Davidovich, and S. Haroche, Phys. Rev. Lett. **76**, 1800 (1996).
[3] D. M. Meekhof, C. Monroe, B. E. King, W. M. Itano, and D. J. Wineland, Phys. Rev. Lett. **76**, 1796 (1996).
[4] G. Rempe, H. Walther, and N. Klein, Phys. Rev. Lett. **58**, 353 (1987).
[5] R. J. Thompson, G. Rempe, and H. J. Kimble, Phys. Rev. Lett. **68**, 1132 (1992).
[6] A. Blais, R.-S. Huang, A. Wallraff, S. M. Girvin, and R. J. Schoelkopf, Phys. Rev. A **69**, 062320 (2004).
[7] J. P. Reithmaier, G. Sek, A. Löffler, C. Hofmann, S. Kuhn, S. Reitzenstein, L. V. Keldysh, V. D. Kulakovskii, T. L. Reinecke and A. Forchel, Nature **432**, 197 (2004).
[8] L. Amico, R. Fazio, A. Osterloh and V. Vedral, Rev. Mod. Phys. **80**, 517 (2008).
[9] R. J. Glauber, Phys. Rev. **131**, 2766 (1963).
[10] D. F. Walls, Nature **306**, 141 (1983).

Dinàmica de l'entrellaçament en el model de Jaynes-Cummings

Author: Nicolás Landa Baila, nlandaba40@alumnes.ub.edu
Facultat de Física, Universitat de Barcelona, Diagonal 645, 08028 Barcelona, Spain.

Advisor: Maria Moreno Cardoner, maria.moreno@fqa.ub.edu

Resum: L'entrellaçament és al cor de les tecnologies quàntiques i afavoreix el còmput quàntic, la comunicació segura i la detecció ultraprecisa. Es pot generar de manera natural mitjançant les interaccions entre àtoms i llum, on els fotons medien l'entrellaçament entre àtoms. En aquest treball analitzem la dinàmica d'entrellaçament que sorgeix de la interacció entre un àtom de dos nivells i un mode quantitzat únic del camp electromagnètic, descrita pel hamiltonià de Jaynes-Cummings. Preparant el sistema en diferents estats inicials —amb l'àtom inicialment excitat i el camp fotònic en un estat de Fock, coherent o de buit comprimit (squeezed)— calculem l'evolució temporal corresponent i quantifiquem el grau d'entrellaçament entre àtom i llum mitjançant l'entropia d'entrellaçament. Els nostres resultats mostren com l'estadística de fotons influeix en la generació i l'estabilitat de l'entrellaçament.

Paraules clau: Física quàntica de molts cossos, Espai de Hilbert, Principi de superposició, Hamiltonià, Matriu densitat, Entropia
ODSs: (4) Educació de Qualitat, (9) Indústria, Innovació i Infraestructura, (13) Acció climàtica.

Objectius de Desenvolupament Sostenible (ODSs o SDGs)

1. Fi de la es desigualtats		10. Reducció de les desigualtats	
2. Fam zero		11. Ciutats i comunitats sostenibles	
3. Salut i benestar		12. Consum i producció responsables	
4. Educació de qualitat	X	13. Acció climàtica	X
5. Igualtat de gènere		14. Vida submarina	
6. Aigua neta i sanejament		15. Vida terrestre	
7. Energia neta i sostenible		16. Pau, justícia i institucions sòlides	
8. Treball digne i creixement econòmic		17. Aliança pels objectius	
9. Indústria, innovació, infraestructures	X		

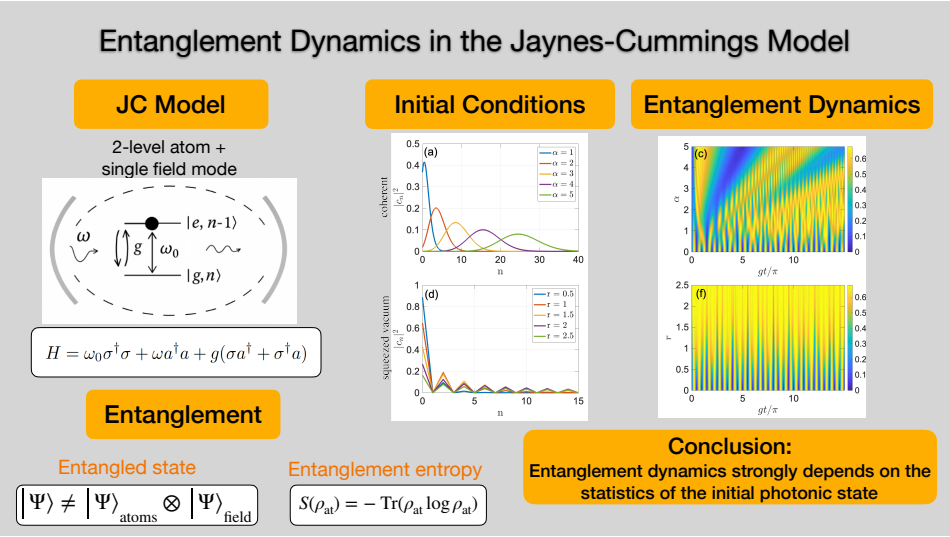

FIG. 4: Abstract Visual